Article

Journal of
Nanoscience and Nanotechnology
Vol. 19, 2130–2137, 2019
www.aspbs.com/jnn

Copyright © 2019 American Scientific Publishers
All rights reserved
Printed in the United States of America

Systematic Toxicity Evaluations of High-Performance Carbon "Quantum" Dots

Jia-Hui Liu[1,*], Yanli Wang[2,*], Gui-Hua Yan[2], Fan Yang[3], Haidi Gao[1], Yanan Huang[2], Haifang Wang[2,*], Ping Wang[3], Liju Yang[4,*], Yongan Tang[5], Lindsay Rose Teisl[3], and Ya-Ping Sun[3,*]

[1] *Beijing Key Laboratory of Bioprocess, College of Life Science and Technology, Beijing University of Chemical Technology, Beijing 100029, China*
[2] *Institute of Nanochemistry and Nanobiology, Shanghai University, Shanghai 200444, China*
[3] *Department of Chemistry and Laboratory for Emerging Materials and Technology, Clemson University, Clemson, South Carolina 29634, USA*
[4] *Department of Pharmaceutical Sciences, Biomanufacturing Research Institute and Technology Enterprise, North Carolina Central University, Durham, North Carolina 27707, USA*
[5] *Department of Mathematics and Physics, North Carolina Central University, Durham, North Carolina 27707, USA*

Carbon dots (CDots) in a general structure of small carbon nanoparticles with various surface passivation schemes have emerged to represent a new class of carbon nanomaterials in now a rapidly advancing and expanding research field. Among various synthesis methods, the use of pre-processed and selected small carbon nanoparticles for deliberate chemical functionalization of the particle surface with organic molecules have produced high-performance and structurally better defined CDots. Specifically, small organic molecules 2,2′-(ethylenedioxy)bis(ethylamine) and 3-ethoxypropylamine were used for the effective surface passivation of the carbon nanoparticles via chemical functionalization to yield CDots that are brightly fluorescent and also structurally ultra-compact, amenable to various desired cell imaging applications. Thus, a systematic evaluation of these CDots on their cytotoxicity profiles is necessary, and performed in this study by using a diverse selection of cell lines. Also for fluorescence imaging, CDots were modified with their encapsulating selected organic dyes for much enhanced red/near-IR fluorescence emissions. These modified CDots with the dyes as guest were also evaluated for their cytotoxicity profiles. The results suggest that the CDots without and with the guest dyes are generally nontoxic to the selected cell lines, further supporting the notion that CDots can be used as high-performance yet nontoxic bioimaging agents.

Keywords: Carbon Dots, Cytotoxicity, Host-Guest.

1. INTRODUCTION

Since the discovery of fullerenes, carbon nanomaterials in different categories have been pursued extensively for their unique characteristics and advantageous properties, which promise a wide variety of technological applications. For example, fullerene derivatives have become popular materials in organic solar cells,[1,2] carbon nanotubes in transparent conductive coatings critical to the development of flexible optoelectronic devices[3,4] and in a number of energy storage systems,[5,6] and graphenes and graphene oxides that compete with fullerenes and carbon nanotubes in many of the same uses and more.[7,8] However, the extraordinary promises of carbon nanomaterials have been accompanied by major concerns on their potential toxicities and the associated transmission mechanisms through the environment.[9–15] Despite the large number of published toxicity evaluations on the carbon nanomaterials in various configurations, debates on some of the major toxicity concerns are still ongoing.[14,15]

Carbon "quantum" dots, or more appropriately named as carbon dots (CDots, Fig. 1)[16–18] for the lack of classical quantum confinement, have emerged to represent a new class of carbon nanomaterials in now a rapidly advancing and expanding research field, as made evident by the extensive recent publications in the literature.[19–28] Generally, CDots are defined as small carbon nanoparticles with various surface passivation schemes (Fig. 1).[16,20,28] Among methods for their syntheses, the use of

*Authors to whom correspondence should be addressed.

 1533-4880/2019/19/2130/008 doi:10.1166/jnn.2019.15807

pre-processed and selected small carbon nanoparticles for deliberate chemical functionalization of the particle surface with organic molecules,[29–31] commonly referred to as the deliberate chemical functionalization method,[28] yields CDots that should structurally more closely adhere to the general definition (Fig. 1). For example, such a synthesis was used successfully to prepare brightly fluorescent CDots of the oligomeric polyethylene glycol diamine (PEG_{1500N}) for surface functionalization, with the optical performance of the resulting PEG_{1500N}-CDots comparing favorably to that of the well-established semiconductor CdSe/ZnS quantum dots in the selected spectral region,[29–32] yet nontoxic to cells and mice according to several investigations.[33–36] More recently, small organic molecules including 2,2′-(ethylenedioxy)bis(ethylamine) (EDA) and 3-ethoxypropylamine (EPA) were used to functionalize carbon nanoparticles for the EDA-CDots and EPA-CDots, which are not only similarly bright in fluorescence emissions but also structurally compact and better defined,[30, 31] thus even more closely adhering to the general definition of CDots. These CDots may serve as ultra-compact fluorescence probes in some of the more demanding cell imaging uses,[37] and also as benchmarks for other dots obtained from the deliberate chemical functionalization synthesis as well as references for those prepared in other synthesis schemes.[19–28, 38, 39] In this regard, toxicity profiles of the CDots with EDA and EPA for surface functionalization and passivation are of significant interest.

Another more popular method for CDots has been the carbonization synthesis with organic species as precursors in often "one-pot" processing.[19–28, 39–41] Toxicity evaluations of the CDots thus produced have generally suggested their being nontoxic.[19, 21–28, 40, 41] Recently, the same synthetic strategy has been employed in the preparation of the carbon-based hybrid nanostructures that are configuration-wise equivalent to CDots with other species as guests embedded in the carbon nanoparticle cores, dubbed as host-guest CDots or G@CDots (G denoting the guest, Fig. 1).[42] The host-guest configuration, with potentially an extremely wide variety of guest selections for different functions and purposes, represents a substantial expansion with respect to the properties and applications of CDots. For red/near-IR emissive organic dye nile blue (NB) as guest, as an example, the NB@CDots exhibited much enhanced fluorescence performance in aqueous media in comparison with that of either free nile blue or the corresponding neat CDots, enabling more effective cell labeling and imaging over the red/near-IR spectral region.[43] Since the host-guest CDots represent a new platform of carbon-based hybrid nanostructures, a systematic evaluation of their toxicity profiles is obviously justified and timely.

In this study, we evaluated the EDA-CDots, EPA-CDots, EDA&EPA-CDots (CDots with surface co-functionalization of EDA and EPA molecules), CV@CDots (CV = cresyl violet), and NB@CDots for their cytotoxicity profiles based on cancer cells (HeLa), normal cells (human gastric mucosal epithelial cell line GES-1), and mesenchyal stem cells (MSCs) and neural stem cells (NSCs). The different cell lines were selected as typical cancer cells, normal cells, and stem cells. The results have suggested that these CDots of different structures, compositions and configurations, and surface functionalities are generally nontoxic to cells.

2. EXPERIMENTAL DETAILS

2.1. Materials

The carbon nanopowder sample was supplied by US Research Nanomaterials. 3-Ethoxypropylamine (EPA) was purchased from TCI, 2,2′-(ethylenedioxy)bis(ethylamine) (EDA) and thionyl chloride from Alfa Aesar, nile blue (sulfate salt) from Chem-Impex International, cresyl violet from Acros Organics, and oligomeric polyethylene glycol (average molecular weight ∼900) from Fluka. Nitric acid was obtained from Fisher Scientific. Dialysis membrane tubing (molecular weight cutoff ∼500 or ∼1,000) was acquired from Spectrum Laboratories. Water was deionized and purified by being passed through a Labconco WaterPros water purification system.

2.2. Measurement

UV/vis absorption spectra were recorded on a Shimadzu UV2501-PC spectrophotometer. Fluorescence spectra were acquired on a Jobin-Yvon emission spectrometer equipped with a 450 W xenon source, Gemini-180 excitation and Triax-550 emission monochromators, and a photon counting detector (Hamamatsu R928P PMT at 950 V). 9,10-Bis(phenylethynyl)-anthracene in cyclohexane and rhodamine 6G in ethanol were used as fluorescence standards in the determination of fluorescence quantum yields by the relative method (matching the absorbance at the excitation wavelength between the sample and standard solutions and comparing their corresponding integrated total fluorescence intensities). FT-IR spectra were measured on a Shimadzu IRAffinity-1S spectrophotometer with the Single Reflection ATR accessory for solid samples.

2.3. CDots with EDA and EPA

For the small carbon nanoparticles, a commercially acquired carbon nanopowder sample (2 g) was refluxed in aqueous nitric acid (8 M, 200 mL) for 48 h. The reaction mixture was cooled to room temperature, and centrifuged at 1,000 g to discard the supernatant. The residue was re-dispersed in deionized water, dialyzed in a membrane tubing (molecular weight cut-off ∼500) against fresh water for 48 h, and then centrifuged at 1,000 g to retain the supernatant. Upon the removal of water, small carbon nanoparticles were recovered for them to be used in the functionalization reactions.[30, 31]

The nanoparticles obtained above were refluxed in neat thionyl chloride for 12 h. The excess thionyl chloride was

IP: 185.223.161.87 On: Thu, 10 Oct 2019 15:39:02
Copyright: American Scientific Publishers
Delivered by ingenta

removed, and the treated sample (50 mg) was mixed well with EDA (1 g) or EPA (1 g) in a round-bottom flask, heated to 120 °C or 110 °C, respectively, and vigorously stirred under nitrogen protection for 72 h. The reaction mixture was cooled to room temperature, dispersed in water, and then centrifuged at 20,000 g to retain the supernatant, followed by dialysis in a membrane tubing (molecular weight cut-off ∼500) against fresh water to yield the EDA-CDots or EPA-CDots in an aqueous solution.

Similarly in the preparation for the EDA&EPA-CDots, the carbon nanoparticles (50 mg) post-treatment with thionyl chloride were mixed well with EPA (1 g), and the mixture was heated to 110 °C for 48 h. Then, EDA (0.6 g) was added, and the resulting mixture was reacted at 120 °C for another 24 h. The reaction mixture was processed in the same centrifugation and dialysis procedures to obtain the EDA&EPA-CDots in an aqueous solution.

2.4. CV@CDots and NB@CDots

In the synthesis of CV@CDots, cresyl violet (CV, 20 mg) in an ethanol solution was mixed well with oligomeric PEGs of molecular weight ∼900 (PEG900, 2 g), followed by the removal of ethanol via purging with nitrogen gas. The resulting mixture was placed in a commercial microwave oven and irradiated at 300 W for 20 min. Then, water was added to the reaction mixture with sonication to obtain a dark colored aqueous solution. The solution was centrifuged at 20,000 g, from which only a negligible amount of precipitate was observed and discarded. The supernatant was dialyzed in a membrane tubing (cutoff molecular weight ∼1,000) against fresh water to remove unreacted starting materials and other small molecular species, yielding CV@CDots in an aqueous solution.

For NB@CDots, nile blue (100 mg) in ethanol (2 mL) was mixed with the PEGs (1 g), and the mixture was sonicated in a bath sonicator (VWR 250D) at 40 °C for 30 min. Then, ethanol was removed by purging the mixture with nitrogen gas. In the preparation for carbonization processing, SiC powders (170 g) in a silica crucible casting dish were heated in a conventional microwave oven at 500 W for 3 min. The small glass container with the reactant mixture was buried in the preheated SiC powders in the microwave oven for irradiation at 1,000 W. The initial microwave processing time was 2 min, and additional processing time was added based on the carbonization outcome. The degree of carbonization was monitored by measuring the absorbances at 400 nm (A400 nm) and 550 nm (A550 nm), and the A400 nm/A550 nm ratio of about one was targeted as the end point for the microwave processing. The processed sample back at room temperature was dispersed in deionized water (10 mL) with sonication in a bath sonicator for 30 min, followed by centrifugation at 20,000 g to keep the supernatant, and then dialysis against fresh water to obtain the NB@CDots in an aqueous solution.

2.5. Cell Viability Evaluations

The CCK-8 assay was used with all cell lines. The cell viability (% of the control) is expressed as the percentage of (ODtest − ODblank)/(ODcontrol − ODblank), where ODtest denotes the optical density (OD) of cells exposed to CDots, ODcontrol the OD of the control, and ODblank the OD without cells.

2.6. Cell Morphology

In 96-well plates, the cells were plated at 6×10^3 cells per well, and incubated for 24 h. Then, the cells were incubated in fresh culture medium containing the different CDots for 24 h. The cell morphology was recorded under an optical microscopy.

2.7. HeLa Cells Incubation

Human epithelial cervical cancer HeLa cells were obtained from the Cell Bank of Chinese Academy of Sciences (Shanghai, China). The cells were maintained in high glucose Dulbecco's Modified Eagle's Medium (DMEM, 4.5 g/L glucose) supplemented with 10% fetal bovine serum (FBS, PAN-biotech GmbH, Germany) and 1% penicillin/streptomycin, and cultured at 37 °C in a humidified atmosphere with 5% CO_2 and 95% air. In 96-well plates, the cells were plated at 6 × 103 cells per well, and incubated for 24 h. Then, the cells were incubated in fresh culture medium containing the different CDots for 24 h. After removing culture medium, the cell viability was evaluated by a WST-8 cell counting kit (CCK-8, Dojindo, Kumamoto, Japan). Briefly, CCK-8 solution (100 μL, containing 10% CCK-8) was added to cells and incubated for 1 h at 37 °C under 5% CO_2 and 95% air. The optical density (OD) of each well at 450 nm was recorded on a microplate reader (Thermo, Varioskan Flash, Waltham, MA, USA) for the determination of cell viability.

IP: 185.223.161.87 On: Thu, 06 Dec 2018 13:26:02
Copyright: American Scientific Publishers
Delivered by Ingenta

2.8. GES-1 and NSCs Incubation

The gastric epithelial GES-1 cells and NSCs (neural stem cells) were provided by the Chinese Academy of Sciences. The cells were grown to confluence in 25 cm^2 flasks supplemented with high-glucose DMEM and 10% fetal bovine serum, and incubated in a humidified incubator with 5% CO_2 and 95% air at 37 °C. Cells of 80% in confluence were used in the CCK-8 assay. Briefly, the cells were seeded in 96-well plates (5×10^3 cells per well), and precultured in culture medium containing the CDots of different concentrations for 24 h. The OD of each well at 450 nm was measured by using a microplate reader for the determination of cell viability.

2.9. MSCs Incubation

The SD rat mesenchymal stem cells (MSCs, OriCellTM Cyagen Biosciences, Inc., Santa Clara, CA) from passage 2 (OriCell Sprague–Dawley rat MSCs, Cyagen) were expanded in SD rat MSC basal media with 10% fetal

bovine serum and 1% v/v penicillin/streptomycin. The MSCs within passage 8 were used in all experiments. For the CCK-8 assay, the cells were re-suspended in the medium at 1.0×10^5 cells/mL, and seeded in a 96 well plate. After 24 h culturing, the cells were exposed to different concentrations of the CDots. After 24 h culturing, 0.1 mL of CCK-8 was added to each well to determine the cell viability.

3. RESULTS AND DISCUSSION

The EDA-CDots, EPA-CDots, and EDA&EPA-CDots (Fig. 1) were prepared by chemical functionalization of pre-processed and selected small carbon nanoparticles with EDA and EPA molecules under amidation reaction conditions.[30,31] For the small carbon nanoparticles, a commercially acquired carbon nanopowder sample was refluxed in aqueous nitric acid for purification and particle surface oxidation with the formation of carboxylic acid moieties, coupled with dialysis to remove oxidized impurities and other species. In the subsequent separation of the aqueous dispersed carbon nanoparticles in terms of centrifugation, smaller particles of more significant surface oxidation were retained in the supernatant, and harvested for the functionalization reactions.

The functionalization of the small carbon nanoparticles with EDA and EPA in amidation reactions for the EDA-CDots and EPA-CDots, respectively, was basically the same as what was reported previously.[30,31] EDA is a diamine, so the EDA-CDots contain a significant number of amine groups on the dot surface, and as a result the dot solution in neutral water is basic (pH around 10–12 depending on concentration). In an aqueous buffer such as PBS, the EDA-CDots are positively charged on the dot surface, potentially hindering their cellar uptakes in some cell imaging and related uses.[37] On the other hand, EPA is a simple amino molecule, and the EPA-CDots in an aqueous solution are close to neutral pH for a lack of free amino moieties on the dot surface (Fig. 1). As reported,[31] the EPA-CDots are more fluorescent than EDA-CDots. However, amino groups on the surface of CDots are useful in terms of further functionalization to attach species designed for specific targeting and related purposes. Thus, CDots co-functionalized with EDA and EPA (EDA&EPA-CDots) were designed and prepared for a combination of the advantageous characteristics of the EDA-CDots and EPA-CDots.

Delivered by Ingenta

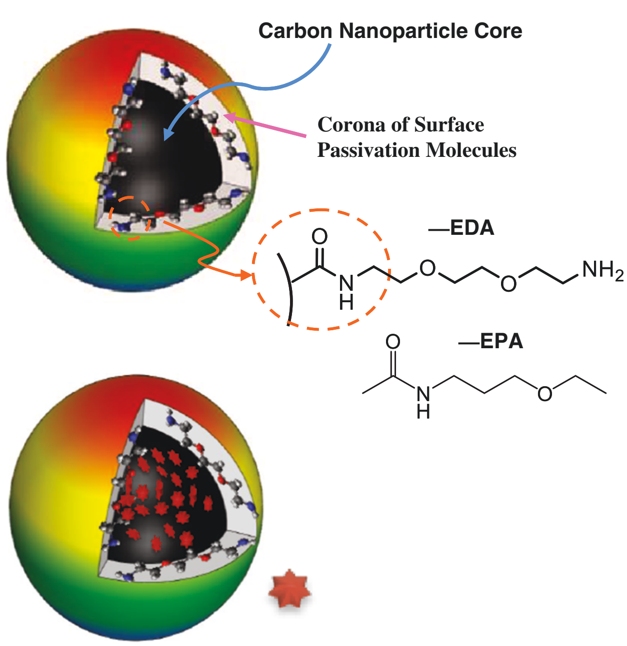

Figure 1. (a) A cartoon illustration on CDots, each of which is generally a small carbon nanoparticle core with attached surface passivation molecules in a configuration similar to a soft corona. The EDA-CDots and EPA-CDots are shown, and the EDA&EPA-CDots may be similarly understood. (b) The NB@CDots and CV@CDots with oligomeric PEGs for surface passivation.

In the synthesis of the EDA&EPA-CDots, the pre-processed and selected small carbon nanoparticles were treated with thionyl chloride, followed by the reaction with EDA and EPA under two different conditions, one in a EDA-EPA mixture and the other with EPA first and then the addition of EDA to continue the reaction. Under the former, the apparently more efficient reaction with EDA made the EDA population on the dot surface overwhelmingly high, with little presence of EPA. Thus, the latter condition was used such that the carbon nanoparticles post-treatment with thionyl chloride were first reacted with neat EPA for a selected period of time, and then EDA in a smaller amount than EPA was added to continue the reaction for a shorter time period than what was initially for EPA. The as-synthesized sample was similarly cleaned via dialysis to remove unreacted EDA, EPA and other unwanted small molecular species to yield the EDA&EPA-CDots in an aqueous solution. In a comparison of acidity in similar solutions, the pH of the EDA-CDots was about 10, the EPA-CDots about 7.5, and the EDA&EPA-CDots about 9. As shown in Figure 2, the UV/vis absorption spectrum of the EDA&EPA-CDots contains some of the special

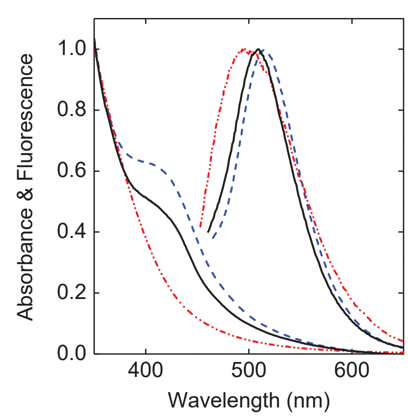

Figure 2. UV/vis absorption spectra (ABS) and fluorescence emission spectra (FLSC, 440 nm excitation) of the EDA-CDots (-·-), EPA-CDots (---), and EDA&EPA-CDots (—) in aqueous solutions.

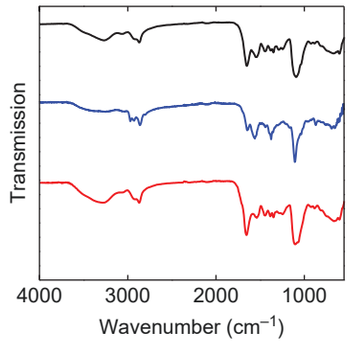

Figure 3. FT-IR spectra of the EDA-CDots (black), EPA-CDots (blue), and EDA&EPA-CDots (red).

absorption features found in the EPA-CDots,[31] suggesting substantial contributions of EPA as co-surface passivation species with EDA in these dots.

FT-IR spectra of the EDA-CDots, EPA-CDots, and EDA&EPA-CDots are rather similar (Fig. 3), largely as expected considering the structural similarities between EDA and EPA (Fig. 1). The terminal amino groups in the dots with EDA on the surface are reflected by the more pronounced broad absorption around 3,300 cm^{-1} in the corresponding spectra (Fig. 3).

The aqueous solutions of EDA-CDots, EPA-CDots, and EDA&EPA-CDots are all very stable, without any precipitations over time. Their UV/vis absorptions in solution (Fig. 2) are due to the surface-functionalized core carbon nanoparticles in the dots, as the organic species for the functionalization are by themselves optically transparent in the near-UV and visible spectral regions. Interestingly, the special surface passivation effects found in the EPA-CDots, which as reported previously[31] are responsible for the extra absorptions in the blue spectral region (Fig. 2), are apparently still significant even in the presence of co-surface passivation agent EDA in the EDA&EPA-CDots. The results also support the earlier conclusion that the special absorption features in the EPA-CDots are due likely to changes in optical transitions associated with altered electronic structures on the EPA-functionalized/modified surface of the core carbon nanoparticles in the dots, not to the creation of any new species in the dot synthesis under the rather mild experimental conditions.[31]

All these dots are brightly fluorescent (Fig. 2), with the spectral region of the strongest emissions overlapping that of the green fluorescent protein.[30,31] Relatively, the EPA-CDots are generally more fluorescent than the EDA-CDots with excitation at 400–450 nm due to the special surface passivation effects in the former, as reported previously,[31] and the EDA&EPA-CDots is apparently between the two in terms of fluorescence brightness and quantum yields (25%), again consistent with the UV/vis absorption results discussed above.

The CDots were evaluated in cytotoxicity assays with cell lines including HeLa cells and MSCs. For HeLa cells

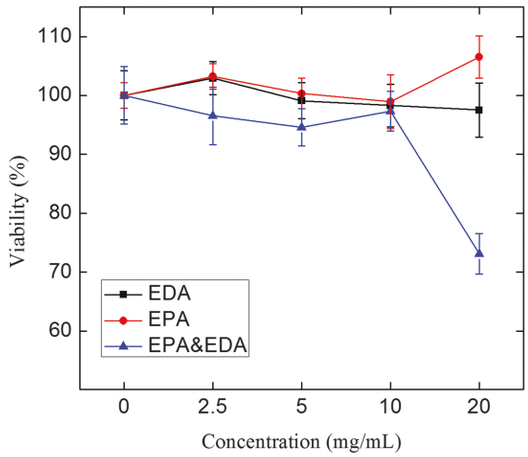

Figure 4. The viability of HeLa cells treated with the EDA-CDots, EPA-CDots, and EDA&EPA-CDots at different concentrations for 24 h.

with the cell viability assay CCK-8, which evaluates the mitochondrial activities of the cells, the three CDots at concentrations up to 20 mg/L (significantly higher than those typically used in cell imaging experiments) were incubated with the cells for 24 h. The cell viabilities were essentially unchanged, except for the EDA&EPA-CDots at the highest concentration tested (Fig. 4). The exception is somewhat surprising because the cytotoxicity of CDots has been thought to be dominated by the surface functionalization species,[35,44] and here the difference is between a EDA-EPA mixture and EDA or EPA only. Even though it is only at the high dot concentration, the apparently somewhat different behavior may be probed in further investigations for a better understanding. The Morphology of Hela cells exposed to 20 mg/L EDA-CDots, EPA-CDots and EDA&EPA-CDots were recorded in Figure 5. The cell density and the cell morphology were not changed by the three CDots exposure.

The same CCK-8 assay was used with MSCs to determine the cell viability after incubation with the EDA-CDots and EPA-CDots. Throughout the dot concentrations tested, the cell viability was essentially unchanged (Fig. 6), suggesting excellent biocompatibility of these CDots to MSCs.

The CDots with EDA and EPA for surface passivation were developed for their ultra-compact dot profiles and bright fluorescence emissions in the green spectral region overlapping that of the green fluorescent protein.[30,31,37] For enhanced fluorescence performance in the red/near-IR to overcome various background signals in bioimaging and sensing, a new platform of CDots with a host-guest configuration (Fig. 1) has been developed recently.[42,43] Among more established host-guest CDots are those with cresyl violet (CV) or nile blue (NB) as the guest, CV@CDots or NB@CDots, respectively. These dots were prepared by the carbonization processing with oligomeric PEGs as the primary carbon source and also the surface passivation

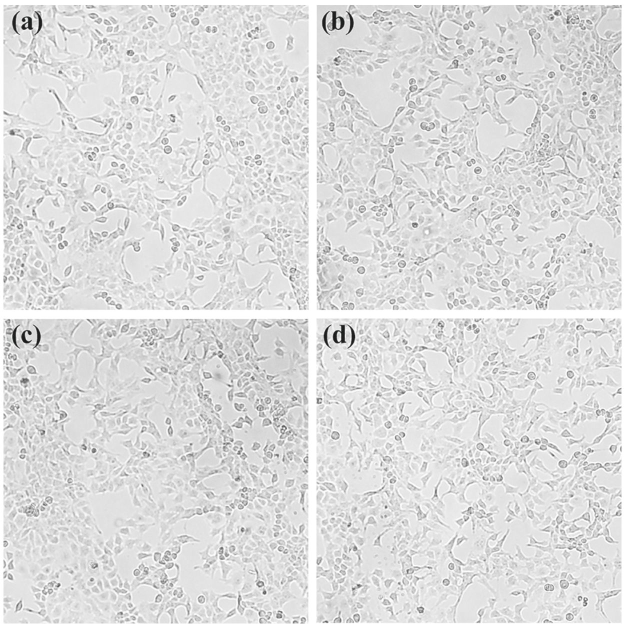

Figure 5. The morphology of HeLa cells treated with the EDA-CDots (b), EPA-CDots (c), and EDA&EPA-CDots (d) at different concentrations and control (a) for 24 h.

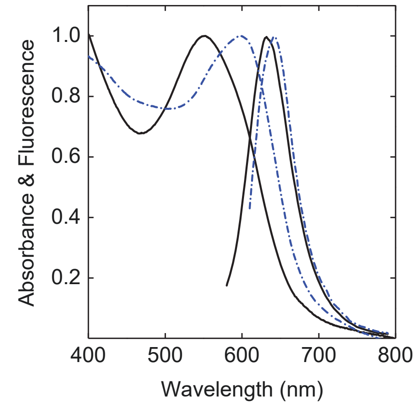

Figure 7. Optical absorption spectra (ABS) and fluorescence emission spectra (FLSC) of the NB@CDots (—) and CV@CDots (-·-) in aqueous solutions.

species in the resulting dots.[42] In this study, the same CV@CDots sample highlighted in the original report[42] and the NB@CDots sample in the recent study[43] were used for cytotoxicity evaluations. Since these dots were designed as red/near-IR fluorescence probes, for referencing purpose their optical absorption and fluorescence spectra are provided and compared in Figure 7.

Human gastric mucosal epithelial GES-1 cells and neural stem cells (NSCs) were used with the CCK-8 assay to compare the viability of the cells after 24 h co-incubation with the CV@CDots and NB@CDots of different concentrations. All of the cell viabilities thus detected are higher than 70% (Figs. 8 and 9), suggesting good biocompatibility of the host-guest CDots. Specifically for the CV@CDots with respect to both GES-1 cells and NSCs, the viability generally decreased with the increasing dot concentration, but little different between the two cell lines (Fig. 8). However, the toxicity of the NB@CDots is apparently somewhat more sensitive to the cell type, without any significant toxicity to GES-1 cells (Fig. 9).

It was shown previously that the NB@CDots were nontoxic to HeLa cells and MSCs,[43] and the repeated experiments in this study reaffirmed the same conclusion. For the CV@CDots, results from the same CCK-8 assay with MSCs suggested generally no changes in cell viability, except for a somewhat improvement at the high dot concentration (Fig. 10). The observation was producible in repeated experiments, thus puzzling. In the literature, there were reports on varying proliferation in cell growth on different substrates, such as composite films of reduced graphene oxides (rGOs) with multiple-walled carbon nanotubes versus common substrates.[45] Similar effects could be in play in the cell viability experiments of CV@CDots, on

Copyright: American Scientific Publishers
Delivered by Ingenta

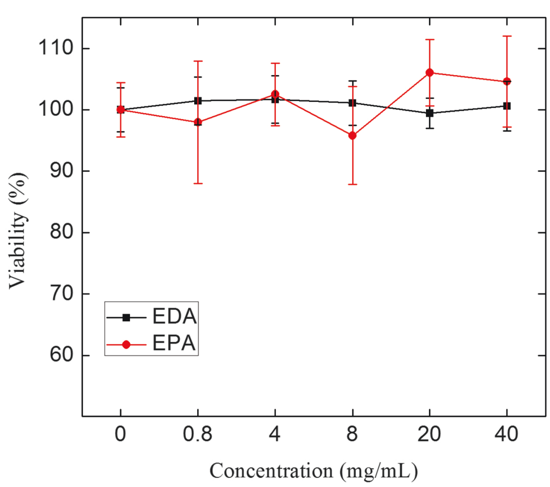

Figure 6. The viability of MSCs treated with the EDA-CDots and EPA-CDots at different concentrations for 24 h.

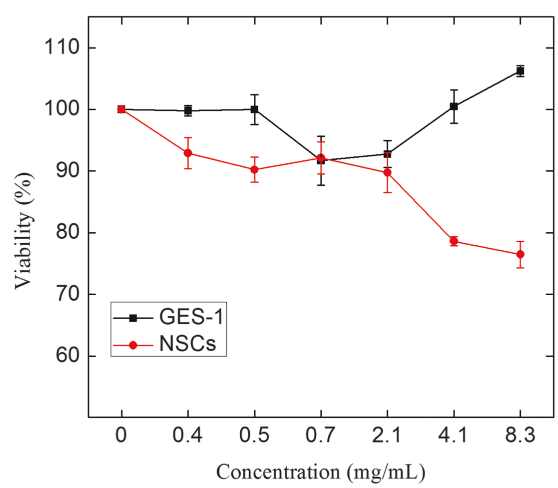

Figure 8. Results from cytotoxicity evaluations of the NB@CDots with GES-1 cells and NSCs at different dot concentrations for 24 h.

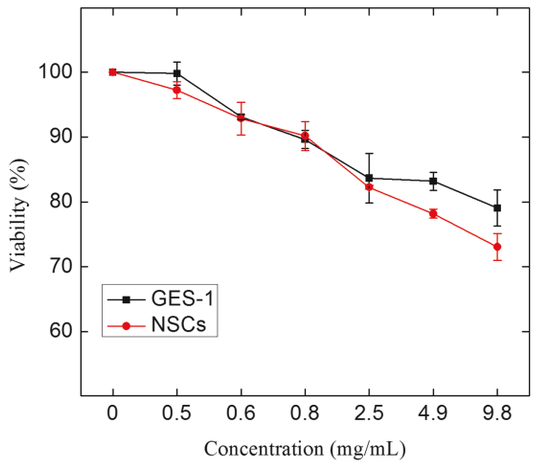

Figure 9. Results from cytotoxicity evaluations of the CV@CDots with GES-1 cells and NSCs at different dot concentrations for 24 h.

which further investigations are required. The Morphology of MSCs exposed to 20 mg/L EDA-CDots, EPA-CDots and CV@CDots were recorded in Figure 11. The cell density and the cell morphology were not changed by the three CDots exposure.

The results presented above suggest that the CDots without and with the guest organic dyes are all generally nontoxic to the selected diverse cell lines at dot concentrations higher than what have typically been used in cell imaging or labeling for fluorescence detection and analyses. Such a conclusion is in general agreement with those on CDots of other surface functionalities and/or from different syntheses,[19, 21–28] supporting the notion that CDots with the relatively simple structure and compositions are intrinsically nontoxic (or no more toxic than the surface functional molecules) to cells. This is particularly significant for the host-guest CDots, which represent a highly versatile expansion of the platform for CDots-derived

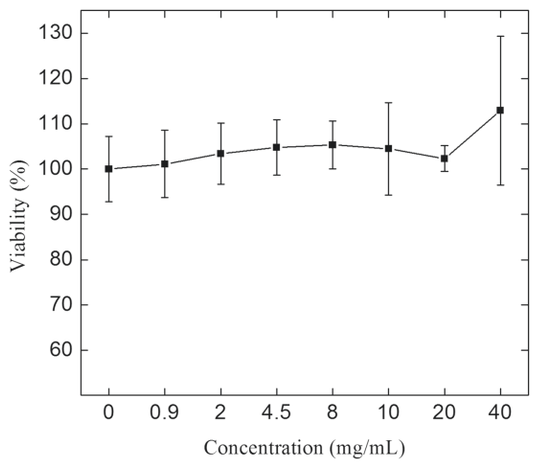

Figure 10. The viability of MSCs treated with the CV@CDots at different concentrations for 24 h.

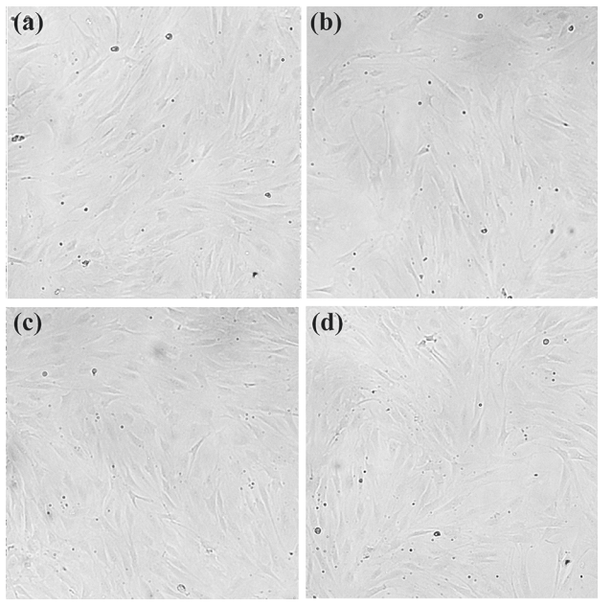

Figure 11. The morphology of MSCs treated with the EDA-CDots (b), EPA-CDots (c), and CV@CDots (d) at different concentrations and control (a) for 24 h.

high-performance fluorescence probes, enabling the effective coverage of red/near-IR spectral regions critical to many biomedical and other applications. Further investigations on the *in vivo* toxicity profiles of these representative CDots in animal models are needed and will be pursued.

4. CONCLUSION

CDots have emerged to represent a new class of carbon nanomaterials in addition to fullerenes, carbon nanotubes, and graphenes, with potentially broad biomedical applications *in vitro* and *in vivo*. In this study, structurally better-defined and ultra-compact CDots including the EDA-CDots, EPA-CDots, and EDA&EPA-CDots (CDots with surface co-functionalization of EDA and EPA molecules) were evaluated for their cytotoxicity profiles, so were the brightly red/near-IR fluorescent host-guest CDots including the CV@CDots and NB@CDots. Based on the use of diverse cell lines including cancer cells (HeLa), normal cells (human gastric mucosal epithelial cell line GES-1), and mesenchyal stem cells (MSCs) and neural stem cells (NSCs), the results have suggested that all these CDots are generally nontoxic, thus supporting the notion that CDots may be considered as similarly high performance yet nontoxic competitors to the presently dominating semiconductor quantum dots.

Acknowledgments: Financial support from NSF DMR1701399 (Liju Yang) and DMR1701424 (Ya-Ping Sun), National Natural Science Foundation of China 21301015 (Jia-Hui Liu) and 21371115 and 11575107 (Yanli Wang), and National Basic Research Program of

China 2016YFA0201600 (Haifang Wang) is gratefully acknowledged.

References and Notes

1. B. C. Thompson and J. M. J. Frechet, *Angew. Chem. Int. Ed.* 47, 58 (**2008**).
2. G. Dennler, M. C. Scharber, and C. J. Brabec, *Adv. Mater*. 21, 1323 (**2009**).
3. S. Roth and H. J. Park, *Chem. Soc. Rev*. 39, 2477 (**2010**).
4. F. Lu, M. J. Meziani, L. Cao, and Y.-P. Sun, *Langumuir* 27, 4339 (**2011**).
5. R. H. Baughman, A. A. Zakhidov, and W. A. de Heer, *Science* 297, 787 (**2002**).
6. L. Dai, D. W. Chang, J.-B. Baek, and W. Lu, *Small* 8, 1130 (**2012**).
7. Y. Zhu, S. Murali, W. Cai, X. Li, J. W. Suk, J. R. Potts, and R. S. Ruoff, *Adv. Mater*. 22, 3906 (**2010**).
8. X. Huang, Z. Yin, S. Wu, X. Qi, Q. He, Q. Zhang, Q. Yan, F. Boey, and H. Zhang, *Small* 7, 1876 (**2011**).
9. S. Kang, M. S. Mauter, and M. Elimelech, *Environ. Sci. Technol*. 43, 2648 (**2009**).
10. B. Nowack, J. F. Ranville, S. Diamond, J. A. Gallego-Urrea, C. Metcalfe, J. Rose, N. Horne, A. A. Koelmans, and S. J. Klaine, *Environ. Toxicol. Chem*. 31, 50 (**2012**).
11. Y. Liu, Y. Zhao, B. Sun, and C. Chen, *Acc. Chem. Res*. 46, 702 (**2013**).
12. J. Zhao, Z. Wang, J. C. White, and B. Xing, *Environ. Sci. Technol*. 48, 9995 (**2014**).
13. J.-H. Liu, T. Wang, H. Wang, Y. Gu, Y. Xu, H. Tang, G. Jia, and Y. Liu, *Toxicol. Res*. 4, 83 (**2015**).
14. E. D. Kuempel, M.-C. Jaurand, P. Moller, Y. Morimoto, N. Kobayashi, K. E. Pinkerton, L. M. Sargent, R. C. H. Vermeulen, B. Fubini, and A. B. Kane, *Crit. Rev. Toxicol*. 47, 1 (**2017**).
15. B. Gholamine, I. Karimi, A. Salimi, P. Mazdarani, and L. A. Becker, *Toxicol. Ind. Health* 33, 1 (**2016**).
16. Y.-P. Sun, B. Zhou, Y. Lin, W. Wang, K. A. S. Fernando, P. Pathak, M. J. Meziani, B. A. Harruff, X. Wang, H. F. Wang, P. G. Luo, H. Yang, M. E. Kose, B. L. Chen, L. M. Veca, and S.-Y. Xie, *J. Am. Chem. Soc*. 128, 7756 (**2006**).
17. Y.-P. Sun, Fluorescent Carbon Nanoparticles, U.S. Pat., 7829772 (**2010**).
18. L. Cao, X. Wang, M. J. Meziani, F. Lu, H. Wang, P. G. Luo, Y. Lin, B. A. Harruff, L. M. Veca, D. Murray, S.-Y. Xie, and Y.-P. Sun, *J. Am. Chem. Soc*. 129, 11318 (**2007**).
19. P. G. Luo, S. Sahu, S.-T. Yang, S. K. Sonkar, J. Wang, H. F. Wang, G. E. LeCroy, L. Cao, and Y.-P. Sun, *J. Mater. Chem. B* 1, 2116 (**2013**).
20. L. Cao, M. J. Meziani, S. Sahu, and Y.-P. Sun, *Acc. Chem. Res*. 46, 171 (**2013**).
21. K. Hola, Y. Zhang, Y. Wang, E. P. Giannelis, R. Zboril, and A. L. Rogach, *Nano Today* 9, 590 (**2014**).
22. Y. Wang and A. Hu, *J. Mater. Chem. C* 2, 6921 (**2014**).
23. P. G. Luo, F. Yang, S.-T. Yang, S. K. Sonkar, L. Yang, J. J. Broglie, Y. Liu, and Y.-P. Sun, *RSC Adv*. 4, 10791 (**2014**).
24. P. Miao, K. Han, Y. Tang, B. Wang, T. Lin, and W. Cheng, *Nanoscale* 7, 1586 (**2015**).
25. S. Y. Lim, W. Shen, and Z. Gao, *Chem. Soc. Rev*. 44, 362 (**2015**).
26. K. A. S. Fernando, S. Sahu, Y. Liu, W. K. Lewis, E. A. Guliants, A. Jafariyan, P. Wang, C. E. Bunker, and Y.-P. Sun, *ACS Appl. Mater. Interfaces* 7, 8363 (**2015**).
27. Y. Du and S. Guo, *Nanoscale* 8, 2532 (**2016**).
28. G. E. LeCroy, S.-T. Yang, F. Yang, Y. Liu, K. A. S. Fernando, C. E. Bunker, Y. Hu, P. G. Luo, and Y.-P. Sun, *Coord. Chem. Rev.* 320, 66 (**2016**).
29. X. Wang, L. Cao, S.-T. Yang, F. Lu, M. J. Meziani, L. Tian, K. W. Sun, M. A. Bloodgood, and Y.-P. Sun, *Angew. Chem. Int. Ed.* 49, 5310 (**2010**).
30. G. E. LeCroy, S. K. Sonkar, F. Yang, L. M. Veca, P. Wang, K. N. Tackett II, J.-J. Yu, E. Vasile, H. Qian, Y. Liu, P. G. Luo, and Y.-P. Sun, *ACS Nano* 8, 4522 (**2014**).
31. F. Yang, G. E. LeCroy, P. Wang, W. Liang, J. Chen, K. A. S. Fernando, C. E. Bunker, H. Qian, and Y.-P. Sun, *J. Phys. Chem. C* 120, 25604 (**2016**).
32. P. Anilkumar, X. Wang, L. Cao, S. Sahu, J.-H. Liu, P. Wang, K. Korch, K. N. Tackett II, A. Parenzan, and Y.-P. Sun, *Nanoscale* 3, 2023 (**2011**).
33. S.-T. Yang, L. Cao, P. G. Luo, F. Lu, X. Wang, H. F. Wang, M. J. Meziani, Y. Liu, G. Qi, and Y.-P. Sun, *J. Am. Chem. Soc.* 131, 11308 (**2009**).
34. S.-T. Yang, X. Wang, H. Wang, F. Lu, P. G. Luo, L. Cao, M. J. Meziani, J.-H. Liu, Y. Liu, M. Chen, Y. Huang, and Y.-P. Sun, *J. Phys. Chem. C* 13, 18110 (**2009**).
35. Y. Wang, P. Anilkumar, L. Cao, J.-H. Liu, P. G. Luo, K. N. Tackett II, S. Sahu, P. Wang, X. Wang, and Y.-P. Sun, *Exp. Biol. Med.* 236, 1231 (**2011**).
36. X. Huang, F. Zhang, L. Zhu, K. Y. Choi, N. Guo, J. Guo, K. Tackett, P. Anilkumar, G. Liu, Q. Quan, H. S. Choi, G. Niu, Y.-P. Sun, S. Lee, and X. Chen, *ACS Nano* 7, 5684 (**2013**).
37. J.-H. Liu, L. Cao, G. E. LeCroy, P. Wang, M. J. Meziani, Y. Dong, Y. Liu, P. G. Luo, and Y.-P. Sun, *ACS Appl. Mater. Interfaces* 7, 19439 (**2015**).
38. Y. Hu, M. M. Al Awak, F. Yang, S. Yan, Q. Xiong, P. Wang, Y. Tang, L. Yang, G. E. LeCroy, X. Hou, C. E. Bunker, L. Xu, N. Tomlinson, and Y.-P. Sun, *J. Mater. Chem. C* 4, 10554 (**2016**).
39. X. Hou, Y. Hu, P. Wang, L. Yang, M. M. Al Awak, Y. Tang, F. K. Twara, H. Qian, and Y.-P. Sun, *Carbon* 122, 389 (**2017**).
40. X. Zhai, P. Zhang, C. Liu, T. Bai, W. Li, L. Dai, and W. Liu, *Chem. Commun.* 48, 7955 (**2012**).
41. Y. Huang, X. Zhou, R. Zhou, H. Zhang, K. Kang, M. Zhao, Y. Peng, Q. Wang, H. Zhang, and W. Qiu, *Chem. Eur. J.* 20, 5640 (**2014**).
42. Y.-P. Sun, P. Wang, Z. Lu, F. Yang, M. J. Meziani, G. E. LeCroy, Y. Liu, and H. Qian, *Sci. Rep*. 5, 12354 (**2015**).
43. P. Wang, J.-H. Liu, H. Gao, Y. Hu, X. Hou, G. E. LeCroy, W. Liang, J. Chen, C. E. Bunker, Y. Liu, and Y.-P. Sun, *J. Mater. Chem. C* 5, 6328 (**2017**).
44. J.-H. Liu, P. Anilkumar, L. Cao, X. Wang, S.-T. Yang, P. G. Luo, H. Wang, F. Lu, M. J. Meziani, Y. Liu, K. Korch, and Y.-P. Sun, *Nano Life* 1 and 2, 153 (**2010**).

Copyright: American Scientific Publishers
Delivered by ingenta

Received: 11 December 2017. Accepted: 12 February 2018.